7. Structural and Luminescence Study of the 3:2 Complex between Europium Nitrate and the B Isomer of Dicyclohexyl-18-crown-6[1])

by **Emmanuel Moret, Francesco Nicolò, Dominique Plancherel, Pascal Froidevaux,** and **Jean-Claude G. Bünzli***

Université de Lausanne, Institut de Chimie Minérale et Analytique, Place du Château 3, CH–1005 Lausanne

and **Gervais Chapuis**

Université de Lausanne, Institut de Cristallographie, BSP, CH–1015 Lausanne

(27.VIII.90)

The crystal and molecular structure of *bis[dinitrato-(2,4,8,15,18,21-hexaoxatricyclo[20.4.0.0^{9,14}]hexacosane)europium(III)]pentakis(nitrato)europiate(III)* $[Eu(NO_3)_2L_B]_2[Eu(NO_3)_5]$), has been determined at 170 K from single-crystal X-ray diffraction. The complex crystallizes in the monoclinic space group $P2_1/n$ (*ITC* No. 14): $a = 16.338(3)$ Å, $b = 15.704(3)$ Å, $c = 24.474(4)$ Å, $\beta = 97.73(1)°$, $Z = 4$. The structure was refined to a final R value of 0.058 ($R_w = 0.060$). The asymmetric unit contains three independent ions lying on general positions: $[Eu(NO_3)_5]^{2-}$and two distinct $[Eu(NO_3)_2L_B]^+$ cations with the macrocyclic ligand in the *cis-anti-cis* conformation (*B*-isomer). The Eu^{III} ions are 10-coordinate with the following mean bond lengths: Eu–O(nitrate) = 2.48(2) Å in the anion and 2.45(2) Å in the two cations, Eu–O(ether) = 2.56(8) and 2.55(5) Å. Small but significant differences are observed between the two complex cations, especially with respect to the positions of the cyclohexyl substituent. A conformational analysis performed on the six O-atoms of the complex cations confirms the predictions of a simple model. The metal ion sites of the complex have been probed by high-resolution excitation and emission spectra at 296 and 77 K. The $^5D_0 \leftarrow {}^7F_0$ excitation spectrum displays two main bands along with several other minor components. A detailed analysis of the corresponding and selectively excited emission spectra leads to the observation of three types of spectra corresponding to the three crystallographically different Eu^{III} ions. Moreover, three minor sites are identified, one anionic and two cationic, with a population equal to *ca.* 10% of the population of the main sites. We interpret this finding as reflecting the presence of molecules with slightly different conformations.

Introduction. – The unique spectroscopic and magnetic properties of the trivalent lanthanide ions make them ideal candidates as probes in various fields of science [2]. In particular, the Eu^{III} ion displays an intense luminescence from a long-lived excited state $^5D_0$ so that high-resolution, laser-excited excitation, and emission spectra of Eu-containing or Eu-doped compounds yield valuable structural and chemical information. In previous work, we have analyzed the number and the local symmetry of the metal ion sites in several macrocyclic complexes [1] [3–9] and shown that the sensitivity of this luminescence method is able to resolve structural differences overseen by X-ray diffraction analyses. The Eu^{III} probe is especially sensitive to small differences in the metal-ion environment [2], a fact we ascertain in this communication in presenting a photophysical study of the 3:2 complex between europium trinitrate and the *cis-anti-cis-B*-isomer (L_B) of *2,5,8,15,18,21-hexaoxatricyclo[20.4.0.0^{9,14}]hexacosane* (dicyclohexyl-18-crown-6, *DC18C6, cf. Fig. 1*). Indeed, *DC18C6* possesses several isomers, five of which have been

[1]) Part 40 of the series 'Complexes of Lanthanoid Salts with Macrocyclic Ligands'; Part 39: [1].

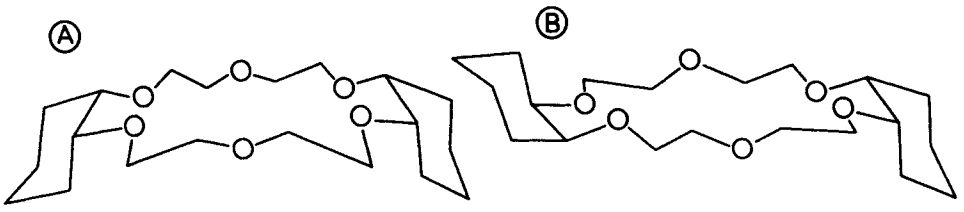

Fig. 1. *Conformation of the* cis-syn-cis (*A*) *and* cis-anti-cis (*B*) *isomers of dicyclohexyl-18-crown-6, L_A and L_B, respectively*

isolated [10]; both L_A and L_B react with lanthanide nitrates to yield 1:1 and 3:2 complexes [11]. Crystal structure determinations have been reported for $[La(NO_3)_3L_A]$ [12], $[Eu(NO_3)_2L_A]_2$ $[Eu(NO_3)_5]$ [13], and $[Ln(NO_3)_2L_B]$ $[Ln(NO_3)_5ONO_2Ln(NO_3)L_B]$, (Ln = La, Pr) [14]. In this communication, we additionally report the crystal and molecular structure of the Eu compound with the *B* isomer in order to check, if the complex dimer reported in the La and Pr structures is also present, and in order to substantiate the conclusions of the photophysical study.

2. Experimental. – *Synthesis and Characterisation of the Complexes.* Europium nitrate was prepared from the oxide (99.99%, *Glucydur*). The ligand L_B was separated from a mixture of *A* and *B* isomers (*Fluka, purum*) by a procedure given in [15]. Its purity was checked by elemental analysis, by its m.p. (67–8°), and by ^{13}C-NMR [13]. The Eu-containing and Eu-doped (2%) Gd complexes were synthesized as described in [13] and gave appropriate elemental analyses.

Luminescence Measurements. Spectra and lifetimes were measured as described in [13] except for the data treatment which was achieved by means of a *W&W SMR* memory recorder (20 MHz, 8 bits) and a *VAX 8550* computer; the decay curves were mathematically treated on an *IBM PS/2 80* computer.

Crystal Data. $C_{40}H_{72}N_9O_{39}Eu_3$, $M = 1758.93$, monoclinic space group $P2_1/n$ (*ITC* No. *14*), $a = 16.338(3)$ Å, $b = 15.704(3)$ Å, $c = 24.474(4)$ Å, $\beta = 97.73(1)°$, $V = 6222(2)$ Å^3, $Z = 4$; $F(000) = 3504$, $D_c = 1.88$, graphite monochromatized MoK_α radiation ($\gamma = 0.71073$ Å), μ(MoK_α) = 30.95 cm^{-1}, $T = 170$ K.

Data Collection and Refinement. Two colourless crystals with dimensions $0.18 \times 0.24 \times 0.35$ mm and $0.15 \times 0.22 \times 0.40$ mm were mounted on a *Syntex R3m* automatic four-circle diffractometer. The cell parameters were obtained from 38 accurately centered reflections with $15 \leq 2\theta \leq 28°$. The intensities of three reference reflections were monitored periodically each 97 measurements. A significant decrease of the standards was observed during the data collection and led us to measure the reflections on limited 2θ ranges. The first 7547 reflections were collected by the $\theta-2\theta$ scan method up to $2\theta = 45°$. At that point, the intensity of the standard reflections had decreased by 25%, and the data collection was continued on a second crystal under the same experimental conditions; 9749 reflections were measured in the range $37 \leq 2\theta \leq 55°$, while the intensity of the standard reflections decreased by 20%. The space group $P2_1/n$ was uniquely determined by the systematic absences *0k0* with *k* odd and *h0l* with $h + l$ odd.

The two sets of intensities, evaluated by the *Lehmann-Larsen* algorithm, were corrected for the decay in intensity and for *Lorentz*-polarization effects; no other corrections were performed. Standard deviations $\sigma(I)$ were estimated from counting statistics, and each set displayed an internal consistence index $R_i = 0.067$. After merging the 2 sets of data, the corresponding value for the 12860 unique reflections was 0.11; 6628 reflections with $I \geq 3.5\ \sigma(I)$ were considered as observed. Atomic scattering factors and dispersion corrections were taken from [16]. The independent Eu-atoms were located from a sharpened three-dimensional *Patterson* map. Initial refinement and completion of the model were carried out by a combination of *Fourier* syntheses and full-matrix least-squares, using bond and angle constraints [13] for the polyether rings. In the final refinement using the block-matrix least-squares method, all non-H-atoms were considered anisotropic without constraints. The H-atoms were included in the model with positions calculated from geometrical considerations (C–H = 0.98 Å) and with a common isotropic displacement parameter refined in each cycle. The model converged to $R_F = 0.058$, $R_w = 0.060$, and G (goodness of fit) = 1.01, with 8 observations per parameter. The weighting scheme used was $1/[\sigma^2(F) + 0.0048*F^2]$. A final difference *Fourier* synthesis showed residual peaks up to 2.4 e/Å^3 in the vicinity of the Eu-atoms (*ca.* 0.9 Å).

Table 1. *Selected Distances* [Å] *and Angles* [°] *with Corresponding e.s.d.'s*

Eu(1)–O(1)	2.715(9)	Eu(2)–O(7)	2.61(1)	Eu(3)–O(52)	2.49(1)
Eu(1)–O(2)	2.52(1)	Eu(2)–O(8)	2.53(1)	Eu(3)–O(53)	2.49(1)
Eu(1)–O(3)	2.53(1)	Eu(2)–O(9)	2.48(1)	Eu(3)–O(62)	2.48(1)
Eu(1)–O(4)	2.502(9)	Eu(2)–O(101)	2.50(1)	Eu(3)–O(63)	2.48(1)
Eu(1)–O(5)	2.59(1)	Eu(2)–O(102)	2.63(1)	Eu(3)–O(72)	2.51(1)
Eu(1)–O(6)	2.50(1)	Eu(2)–O(103)	2.53(1)	Eu(3)–O(73)	2.45(1)
Eu(1)–O(12)	2.414(9)	Eu(2)–O(32)	2.49(1)	Eu(3)–O(82)	2.48(1)
Eu(1)–O(13)	2.477(9)	Eu(2)–O(33)	2.45(1)	Eu(3)–O(83)	2.48(1)
Eu(1)–O(22)	2.463(9)	Eu(2)–O(42)	2.42(1)	Eu(3)–O(92)	2.51(1)
Eu(1)–O(23)	2.44(1)	Eu(2)–O(43)	2.44(1)	Eu(3)–O(93)	2.45(1)
Eu(1)···N(1)	2.93(1)	Eu(2)···N(3)	2.92(1)	Eu(3)···N(9)	2.92(1)
Eu(1)···N(2)	2.87(1)	Eu(2)···N(4)	2.87(1)	Eu(3)···N(8)	2.93(1)
Eu(3)···N(5)	2.92(1)	Eu(3)···N(6)	2.91(1)	Eu(3)···N(7)	2.92(1)
O(5)–Eu(1)–O(6)	63.9(3)	O(32)–Eu(2)–O(33)	51.6(3)	O(22)–Eu(1)–O(23)	52.0(3)
O(3)–Eu(1)–O(4)	62.7(3)	O(92)–Eu(3)–O(93)	51.1(4)	O(101)–Eu(2)–O(102)	61.3(3)
O(1)–Eu(1)–O(6)	63.0(3)	O(72)–Eu(3)–O(73)	51.6(3)	O(8)–Eu(2)–O(9)	63.0(3)
O(12)–Eu(1)–O(13)	51.6(3)	O(52)–Eu(3)–O(53)	51.4(3)	O(7)–Eu(2)–O(8)	60.7(3)
O(102)–Eu(2)–O(103)	63.1(3)	O(4)–Eu(1)–O(5)	59.9(3)	O(42)–Eu(2)–O(43)	52.7(3)
O(9)–Eu(2)–O(101)	62.5(3)	O(2)–Eu(1)–O(3)	64.1(3)	O(82)–Eu(3)–O(83)	51.9(3)
O(7)–Eu(2)–O(103)	64.5(3)	O(1)–Eu(1)–O(2)	60.8(3)	O(62)–Eu(3)–O(63)	51.6(4)
N(1)···Eu(1)···N(2)	174.0(3)	N(5)···Eu(3)···N(8)	94.7(4)	N(7)···Eu(3)···N(8)	120.5(4)
N(5)···Eu(3)···N(6)	177.1(4)	N(5)···Eu(3)···N(7)	96.3(3)	N(6)···Eu(3)···N(9)	99.0(4)
N(7)···Eu(3)···N(9)	119.7(4)	N(3)···Eu(2)···N(4)	175.7(3)	N(6)···Eu(3)···N(8)	84.8(4)
N(5)···Eu(3)···N(9)	78.7(3)	N(8)···Eu(3)···N(9)	119.8(4)	N(6)···Eu(3)···N(7)	86.4(4)
N–O (*nitrate*)	1.25(2)			C–C (*hexyl*)	1.52(2)
C–O (*crown*)	1.43(2)			C–C (*crown*)	1.51(3)
O–N–O (*bite*)	115(1)			C–C–O (*crown*)	106(1)
O–N–O (*no-bite*)	123(1)			C–O–C (*crown*)	114(1)

Table 2. *Selected Least-Square Planes*[a]) *with Deviations* [Å] *and Dihedral Angles* [°]

Plane 1	O(1)*	0.17	O(2)*	0.48	O(3)*	–0.73	O(4)*	0.24	O(5)*	0.38
	O(6)*	–0.63	Eu(1)	0.01	N(1)	2.93	N(2)	–2.96		
Plane 2	N(1)*	–0.02	O(11)*	0.01	O(12)*	0.00	O(13)*	0.01	Eu(1)	0.05
Plane 3	N(2)*	0.01	O(21)*	–0.01	O(22)*	0.00	O(23)*	0.00	Eu(1)	–0.03
Plane 4	O(7)*	0.18	O(8)*	0.48	O(9)*	–0.75	O(101)*	0.30	O(102)*	0.30
	O(103)*	–0.65	Eu(2)	–0.02	N(3)	2.89	N(4)	–2.89		
Plane 5	N(3)*	0.01	O(31)*	0.00	O(32)*	0.00	O(33)*	0.00	Eu(2)	–0.10
Plane 6	N(4)*	0.03	O(41)*	–0.01	O(42)*	–0.01	O(43)*	0.00	Eu(2)	–0.06
Plane 7	Eu(3)*	0.00	N(7)*	0.00	N(8)*	0.00	N(9)*	0.00	O(72)	0.39
	O(73)	–0.45	O(82)	0.56	O(83)	–0.50	O(92)	–0.28	O(93)	0.27
	N(5)	2.86	N(6)	–2.88						
Plane 8	N(5)*	0.00	O(51)*	0.00	O(52)*	0.00	O(53)*	0.00	Eu(3)	0.28
Plane 9	N(6)*	0.01	O(61)*	–0.00	O(62)*	–0.00	O(63)*	0.00	Eu(3)	–0.22

Dihedral angles

1–2	88.4(4)	1–3	88.1(4)	2–3	87.1(6)
1–4	6.9(2)	4–5	87.2(4)	4–6	89.6(4)
5–6	82.5(5)	7–8	74.6(4)	7–9	85.6(5)
8–9	70.8(5)				

[a]) Atoms defining the plane are indicated by *.

The data-reduction, solution of the structure, and the drawings were performed with the SHELXTL-PLUS program package from *Nicolet XRD* (1987). The refinement was carried out with SHELX76 [17] and the geometrical and conformational calculations were done using the PARST program [18]. Selected bond lengths and angles are reported in *Table 1* and mean weighted planes in *Table 2. Supplementary material available*: list of fractional atomic coordinates and equivalent isotropic displacement parameters, list of the anisotropic displacement parameters, list of fractional H-atom coordinates, full list of bond lengths and angles, and list of observed and calculated structure factors (64 pages).

3. Description of the Structure. – The cell dimensions of $[Eu(NO_3)_2L_B]_2[Eu(NO_3)_5]$ are substantially different from those reported for the complex with the *A* isomer [13], even after transformation into the standard $P2_1/c$ space group and despite similar cell volumes. The most significant difference appears in the dimension of the *b* axis, and may be explained by the conformational difference between the macrocyclic ligands leading to a more elongated complex with L_B and to a different crystal packing (*cf. Fig. 2*). The

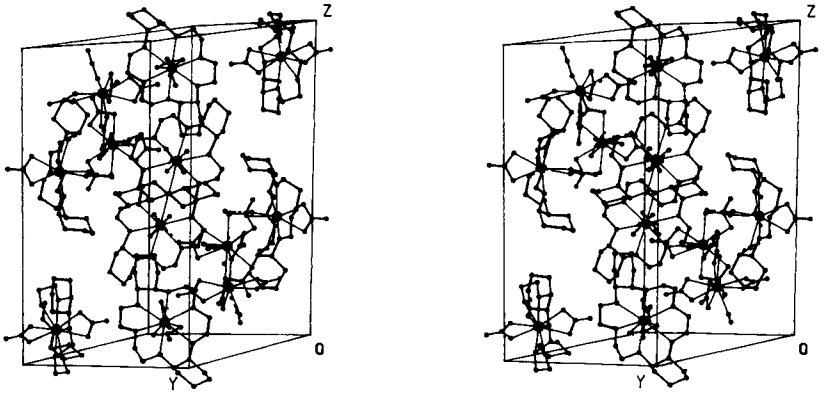

Fig. 2. *Stereoscopic view of the crystal packing in* $[Eu(NO_3)_2L_B]_2[Eu(NO_3)_5]$. The H-atoms have been omitted for clarity.

asymmetric unit consists of three independent ions located on general positions, without local symmetry and with no interaction between them: $[Eu(NO_3)_5]^{2-}$ and two structurally similar $[Eu(NO_3)_2L_B]^+$ complex cations with the polyether in the *cis-anti-cis* conformation. This situation differs from that described for the 3:2 La and Pr complexes with L_B [14] in which one *bis*(nitrato) cation interacts strongly with the Ln ion of the *pentakis*(nitrato) anion, resulting in the presence of one 11-coordinate Ln^{III} ion. In the investigated compound, all three Eu^{III} cations are 10-coordinate, similar to the *A*-isomer analogue [13].

The $[Eu(NO_3)_5]^{2-}$ anion displays a distorted trigonal bipyramidal symmetry with three N-atoms, N(7), N(8), and N(9), on the equatorial plane (plane 7, *cf. Table 2*) and the other two, N(5) and N(6), on an axis approximately normal to this plane (*cf. Fig. 3, Tables 1* and *2*). The idealized symmetry of the N-atom arrangement in *pentakis*(nitrato) species is usually D_{3h} [19], but here the deviation from the idealized geometry is large, especially if angles are considered. A more realistic description would assign a pseudo symmetry C_2 to the N-atom arrangement. The coordination polyhedron around Eu(3) is shown in

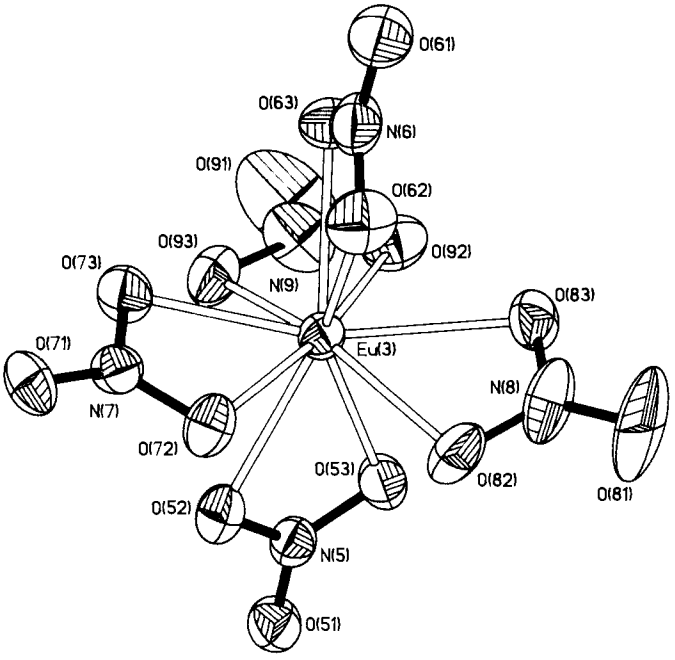

Fig. 3. *Molecular structure at 170 K of the* $[Eu(3)(NO_3)_5]^{2-}$ *anion showing the atom-numbering scheme.* Thermal ellipsoids are drawn at 20% probability.

Fig. 4. Six equatorial O-atoms define an arrangement with a boat conformation, and the remaining four lie pairwise in two planes making dihedral angles of 75 and 86°, respectively, with the plane defined by Eu(3), N(7), N(8), and N(9). The Eu–O bond lengths are all close to the mean Eu–O distance of 2.48(2) Å, resulting in a more homogeneous coordination shell around the metal ion than in the *A*-isomer analogue. Using *Shannon*'s definition [20], the calculated ionic radius of the 10-coordinate Eu^{III} ion is 1.17(2) Å close to the predicted value of 1.178 Å [19].

The two $[Eu(NO_3)_2L_B]^+$ cations are structurally similar, with the Eu-atoms held in the mean plane defined by the O-atoms of the polyether by two bidentate nitrate ions lying in planes perpendicular to the O-atom plane (*Fig. 5*). The crown ether has approximate local symmetry C_{2v} with the pseudo-twofold axis in the mean plane of the polyether; the entire complex moiety has, however, no symmetry element. The two nitrate ions define planes that are almost perpendicular to each other, with dihedral angles of 87 and 82° for Eu(1) and Eu(2), respectively. In the structure of the *A* isomer, the nitrate coordinated on the same side of the cyclohexyl rings was found to be almost parallel to the mean planes of the alkyl substituents and bisecting the dihedral angle between the latter. In $[Eu(NO_3)_2L_B]^+$, one nitrate is perpendicular to the cyclohexyl ring situated on the same side, while the other is more or less parallel to the substituent, generating two sterically different situations for the cyclic alkyl residues. This results in dihedral angles between the O-atom mean plane and the mean planes of the cyclohexyl substituents differing by 25°, the larger angle corresponding to the cyclohexyl next to the perpendicular nitrate.

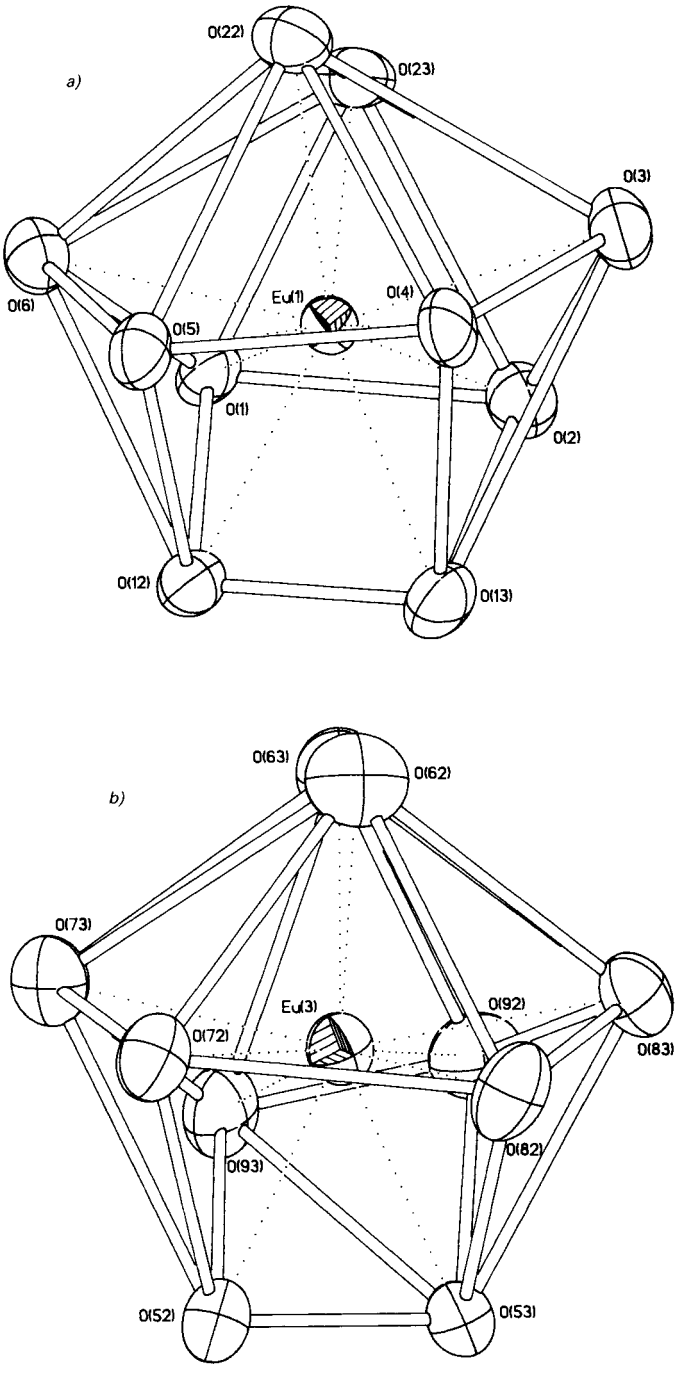

Fig. 4. *Coordination polyhedra of* a) $[Eu(1)(NO_3)_2L_B]^+$ *and* b) $[Eu(3)(NO_3)_5]^{2-}$

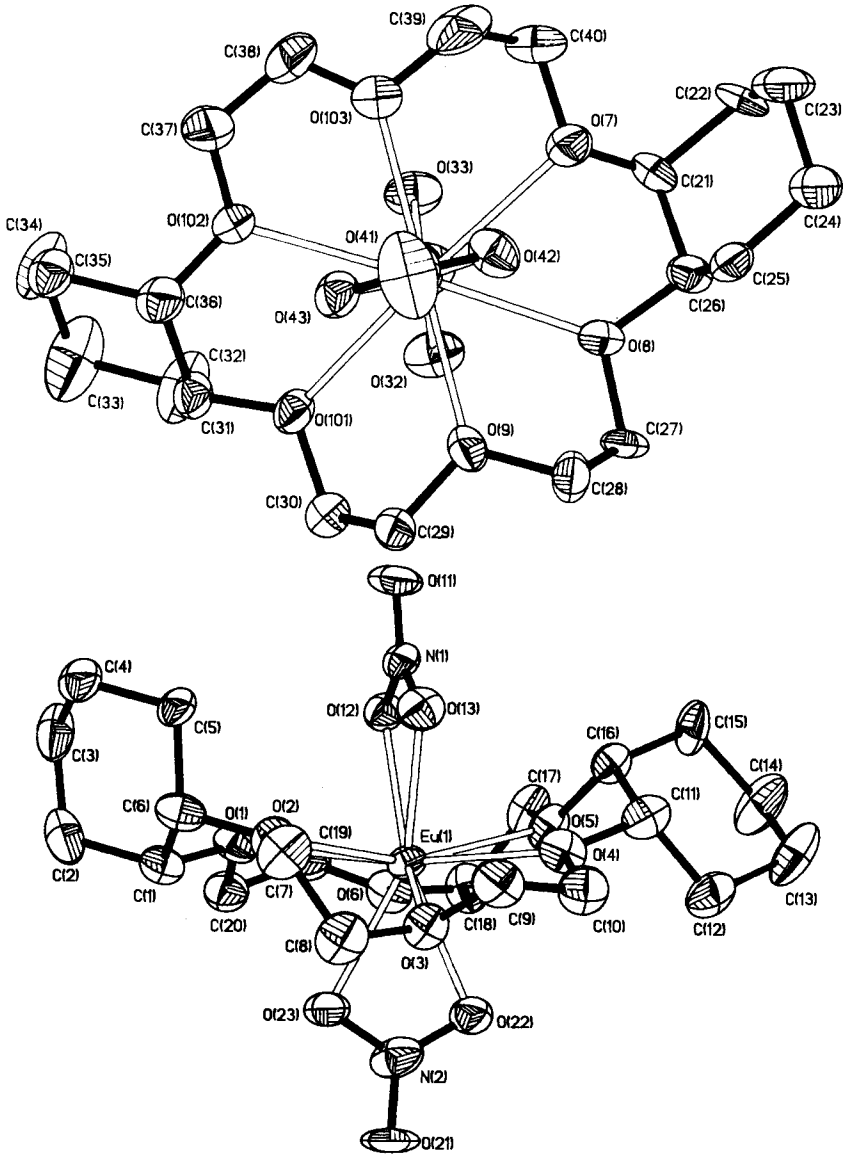

Fig. 5. *Molecular structure at 170 K of the* $[Eu(1)(NO_3)_2L_B]^+$ *cation showing the atom-numbering scheme.* Thermal ellipsoids are drawn at 20% probability.

The two complex cations differ in the conformation of the ligand around Eu(2), with dihedral angles between the O-atom mean plane and the cyclohexyl substituents 18° smaller than for Eu(1). Other differences between the two complex cations are observed upon examination of the Eu-coordination shell. The mean Eu–O(ether) bond lengths are 2.56(8) and 2.55(5) Å for Eu(1) and Eu(2), respectively, but the six bonds are not

equivalent. The Eu–O distances range from 2.50 to 2.71 Å for Eu(1) and from 2.48 to 2.63 Å for Eu(2). In each complex cation, there are two long bonds, 2.71 and 2.59 Å in Eu(1) and 2.61 and 2.63 Å in Eu(2), resulting in an elliptical shape of the polyether cavities. In $[Eu(NO_3)_2L_A]^+$, the mean Eu–O(ether) distance was 2.55(9) Å and the two longer bonds were between Eu^{III} and two opposite O-atoms, while in the complex with L_B these longer bonds are on the same side of the polyether cavity (in *meta*-positions). With respect to these bonds, the complex cations with L_B differ more than the cations containing L_A.

A conformational study similar to that proposed in [13] has been performed on the arrangement of the six O-atoms. Both polyethers display a mean O···O interatomic distance of 2.65 Å identical to the value found for L_A. According to our model (*cf.* Table 3 in [13]), we expect to have a largely puckered boat conformation in $[Eu(NO_3)_2L_B]^+$. Calculation of the geometrical parameters gave θ values of 85 and 82° for Eu(1) and Eu(2), respectively, close to the predicted value of 90°. Furthermore, the Q values proportional to the deviation of the ring from planarity are 1.18 and 1.19, respectively. The estimate of the simple model proposed in our earlier work is, therefore, further confirmed by the presently reported structure.

4. Luminescence Study. – For assignment of the transitions, the excitation and emission spectra have been recorded at 295 and 77 K. Indeed, the intensity of the vibronic transitions decreases at lower temperature, and the emission bands get sharper. The

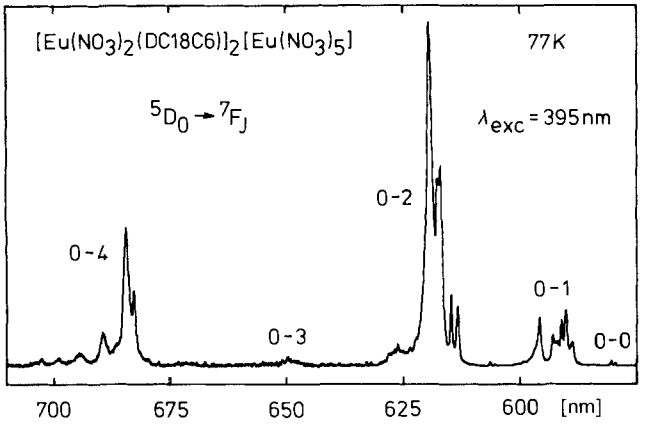

Fig. 6. *Luminescence spectrum of* $[Eu(NO_3)_2L_B]_2[Eu(NO_3)_5]$ *at 77 K under non-selective excitation of the* $^5L_6$ *level* (395 nm)

survey luminescence spectrum (*Fig. 6*) obtained under broad-band excitation to the $^5L_6$ level contains transitions originating almost exclusively from the $^5D_0$ level, along with vibronic transitions. It is dominated by the two electric dipole transitions $^5D_0 \rightarrow {}^7F_2$ and $^5D_0 \rightarrow {}^7F_4$, and the number of components of each $^5D_0 \rightarrow {}^7F_j$ transition reveals the presence of several different metal-ion environments. The weak, forbidden transition between the two non-degenerate $^5D_0$ and $^7F_0$ levels is shown in *Fig. 7*. At 295 K, it is comprised of two comparatively broad bands centered at 17241 and 17263 cm^{-1} (full width at half height *fwhh* = 12 cm^{-1}) which shift to 17230 and 17257 cm^{-1} at 77 K (*fwhh* = 9 cm^{-1}), indicating the presence of at least two different Eu sites. A more sensitive way of studying this

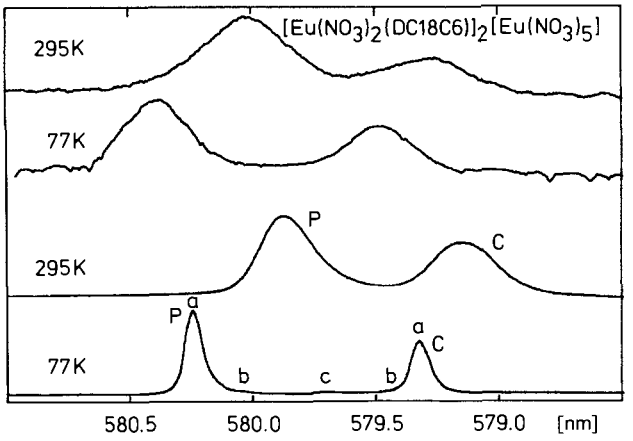

Fig. 7. *Emission* (top two curves) *and excitation spectra of the transition* $^5D_0 \leftrightarrow {}^7F_0$ *in* $[Eu(NO_3)_2L_B]_2[Eu(NO_3)_5]$ *at 295 and 77 K.* Exper. conditions: excitation wavelength 395 nm, analysing band-pass 0.1 nm (top two spectra) and analysing wavelength 590 nm, excitation band-pass 0.03 nm (bottom spectra).

transition is to record it in the exitation mode [2] while monitoring the intense hypersensitive $^5D_0 \rightarrow {}^7F_2$ transition (*Fig. 7*). At 295 K, two components are also observed, at 17245 (P) and 17267 cm^{-1} (C) with *fwhh* = 9 cm^{-1}, but the band labelled P is asymmetric, pointing to the presence of an additional component. At 77 K, the spectrum displays three other minor components in addition to bands P_a (17235 cm^{-1}, *fwhh* = 3 cm^{-1}) and C_a (17261 and 3 cm^{-1}): P_b, C_b, and C_c at 17240, 17257, and 17251 cm^{-1}, respectively. Using an approximate phenomenological relationship between the energy of the $^5D_0 \leftarrow {}^7F_0$ transition and the sum of the formal negative charges of the ligands directly bonded to the Eu^{III} ion [2], we find that bands P and C correspond to charges of −5.1 and −1.9, respectively, pointing to an assignment of P to the $[Eu(NO_3)_5]^{2-}$ anion and of C to the complex cations. We note that P undergoes the expected red shift of *ca.* 10 cm^{-1} upon lowering the temperature to 77 K (1 cm^{-1}/24 K [2]), while band C is less shifted.

To confirm the above assignment, selective excitations of the different Eu^{III} sites to their specific $^5D_0$ levels have been performed, yielding the luminescence spectra reported in *Fig. 8*. These spectra are typical of low-symmetry species, as indicated by the number of components of each $^5D_0 \rightarrow {}^7F_j$ transition and by the relative intensities of these transitions (*Table 3*). The P-type spectra are dominated by a strong $^5D_0 \rightarrow {}^7F_2$ transition, as already reported for other *pentakis*(nitrato) complexes [5] [19]. The C-type spectra have a less intense hypersensitive transition and are similar to those described for *bis*(nitrato) complexes with crown ethers [5–8]; the $^5D_0 \rightarrow {}^7F_1$ transition contains more than 2J + 1 components, pointing to these spectra as being the superposition of two or three different spectra. Differences between P-type and C-type spectra are also examplified by the substantially different shapes displayed by the $^5D_0 \rightarrow {}^7F_5$ and $^5D_0 \rightarrow {}^7F_6$ transitions[2]).

The sharpness of the emission bands at 77 K allows one to perform a detailed study of the spectra and, therefore, to discuss differences occurring in the Eu^{III} environment in both the anionic and cationic species. The excitation wavelength was scanned through the

[2]) Detailed spectra of the $^5D_0 \rightarrow {}^7F_j$ transitions are available upon request from *J.-C. B.*

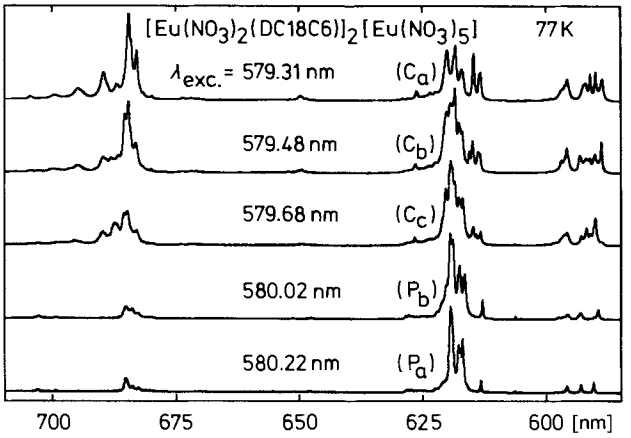

Fig. 8. *Luminescence spectra of* $[Eu(NO_3)_2L_B]_2[Eu(NO_3)_5]$ *at 77 K under selective laser excitation of the* $^5D_0$ *level*

Table 3. *Relative Integrated and Corrected Intensities* (± 10%) *of the* $^5D_0 \rightarrow {}^7F_J$ *Transitions in the Selectively Excited Luminescence Spectra of* $[Eu(NO_3)_2L_B]_2[Eu(NO_3)_5]$ *at 77 K.* Intensities are normalized with respect to the $^5D_0 \rightarrow {}^7F_1$ transition.

J	Band:	C_a	C_b	C_c	P_b	P_a
	λ_{exc} [nm]:	579.31	579.48	579.68	580.02	580.22
1		1.00	1.00	1.00	1.00	1.00
2		2.08	2.99	3.93	11.68	13.24
3		0.09	0.06	0.10	0.07	0.12
4		2.39	2.19	2.14	1.56	2.11
5		0.12	0.09	0.06	0.13	0.22
6		0.89	0.73	0.58	0.54	0.75

profile of the $^5D_0 \leftarrow {}^7F_0$ transition by 0.03-nm increments, and several spectra were obtained in which the emission bands are displaced relative to those observed while exciting at the maxima of bands P and C. Each spectrum corresponds to a different chemical environment for the Eu^{III} ion. Our excitation band-pass was not narrow enough to selectively excite one Eu site only, and each recorded emission spectrum was often a superposition of spectra. By means of spectral subtraction, we could, however, identify the six spectra displayed in *Fig. 9* and corresponding to six Eu^{III} environments, two anionic and four cationic. Since the complex moities are well isolated in the crystal, almost no energy transfer was observed between $[Eu(NO_3)_5]^{2-}$ and $[Eu(NO_3)_2L_B]^+$ upon excitation of the cation. The situation for $[Eu(NO_3)_5]^{2-}$ is relatively simple in that the two spectra P_a and P_b are similar and can be obtained free from interferences due to other species. Spectrum P_a arises from a major species with low symmetry, the crystal field levels of which are reported in *Table 4*, together with the corresponding data for the *pentakis*-(nitrato) species found in the compound with the *A* isomer, $P(L_A)$, [5] and in the tetraphenylarsonium salt (P_{As}) [19]. The barycenters of the ^7F_J levels are similar in all these compounds, *e.g.* $^7F_1$: 363, 370, and 363 cm^{-1}, or $^7F_2$: 1025, 1021, and 1023 cm^{-1}, for $P(L_A)$, P_a, and P_{As} respectively. However, the crystal field splitting is larger for P_a, in line with the large deviation from the idealized geometry evidenced by the X-ray diffraction study. The

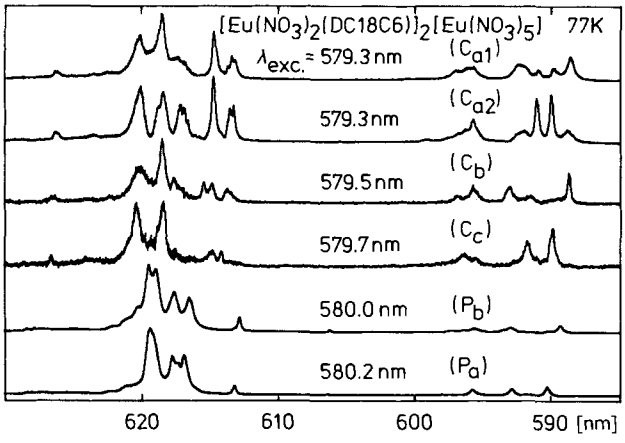

Fig. 9. *$^5D_0 \rightarrow {}^7F_1$ and $^5D_0 \rightarrow {}^7F_2$ transitions in the luminescence spectra of $[Eu(NO_3)_2L_B]_2[Eu(NO_3)_5]$ at 77 K*

Table 4. *Energy* [cm^{-1}] *of the ^7F_J Sublevels (J = 1–4) and of the $^5D_0$ Level of Eu^{III} in $X_2[Eu(NO_3)_5]$ Species as Identified from Luminescence Spectra at 77 K.* The energy of the $^7F_0$ level is taken as origin.

X =	$[Eu(NO_3)_2L_A]^+$ [5]	$[Eu(NO_3)_2L_B]^+$		$[Ph_4As]^+$ [19]
		P_a	P_b	
$^7F_1$	288	294	273	300
	375	368	377	362
	425	449	451	429
$^7F_2$	921	925	921	1010
	1026	1021	1017	1023
	1036	1032	1045	
	1064	1043	1081	1068
	1076	1086	1095	1082
$^7F_3$	1662	1662	1666	1670
	1759	1755	1763	
	1776			1779
	1790	1794	1795	1794
	1824	1818	1817	1803
		1843	1846	1836
	1871	1877	1883	1863
	1965	1967	1969	1947
$^7F_4$	2526	2535	2529	2535
	2571	2576	2586	2568
	2597	2604	2611	2601
	2629	2633	2638	2636
				2908
	2924	2928	2939	2932
	2963	2956	2978	
	3007	3004	3005	2994
$^5D_0$	17232	17235	17240	17224

second spectrum P_b originates from a minor species the population of which is about ten times less than P_a (*vide infra*). It appears to be more distorted than P_a, its crystal field splitting being larger. The presence of this species deserves some comment, since such a secondary species was not observed in the corresponding compound with the *A* isomer. In our study of the 4:3 complexes between europium nitrate and crown ethers, $[Eu(NO_3)_2L]_3[Eu(NO_3)_6]$ [6–8], we have always found that a scan of the excitation wavelength through the profile of the $^5D_0 \leftarrow {}^7F_0$ transition yields series of similar, although distinct spectra. The differences between spectra originating from the *hexakis*(nitrato) anions were, however, very small, and no secondary site similar to P_b could be evidenced. Moreover, in the case of the 18-crown-6 complex the site symmetries derived from the photophysical and the X-ray diffraction studies were not the same, a fact that could be traced back to a particularity of the crystal structure [21]: the centrosymmetric arrangement of the Ln-atoms is destroyed by the conformational disorder of the ligands, and the true space group is polar and not centrosymmetric. As a result, there is a statistical distribution of $[Eu(NO_3)_6]^{3-}$ molecules with conformations having a symmetry close to $2/m$ (C_{2h}), but actually not having an inversion center, since this element is absent from the crystal symmetry. In the compound described here, there is no ambiguity between centrosymmetric and polar space groups, but the crystal packing introduces a large distortion of the $[Eu(NO_3)_5]^{2-}$ anions with respect to their ideal geometry. Owing to small defects which are always present in crystalline materials, some molecules may eventually adopt a more distorted geometry, leading to the observation of the secondary site P_b.

When the excitation wavelength is set on maximum C of the $^5D_0 \leftarrow {}^7F_0$ transition, the resulting emission spectrum presents a $^5D_0 \rightarrow {}^7F_1$ transition with too many components to be assigned as arising from a single crystallographic site (*Fig. 8*). A scan through the excitation profile allowed us to identify two spectra labelled C_{a1} and C_{a2} in *Fig. 9*. We assign these two spectra to the two crystallographically different $[Eu(NO_3)_2L_B]^+$ cations. The latter have indeed very similar Eu environments, the main difference lying in the length of the two long Eu–O bonds (*vide supra*). Since these long bonds have less influence on the crystal field splitting than the regular Eu–O bonds [1], one understands why the two spectra C_{a1} and C_{a2} are difficult to separate. In the case of the *A* isomer, the situation was more complex and five distinct spectra could be distinguished, some of them being a mixture of slightly different spectra; their assignment was done taking into account the disorder found in one of the complex cation. Spectra C_{a1} and C_{a2} are similar to

Table 5. *Energy* [cm^{-1}] *of the* ^7F_J *Sublevels* ($J = 1$–2) *of Eu(III) in* $[Eu(NO_3)_2L_B]^+$ *Species as Identified from Luminescence Spectra at 77 K.* The energy of the $^7F_0$ level is taken as origin.

Level	C_{a1}	C_{a2}	C_b	C_c
$^7F_1$	274	311	270	300
	368	342	394	352
	487	475	469	479
$^7F_2$	953	960	956	965
	989	991	988	981
	1048	1055	1044	1059
	1098	1089	1084	1079
	1137	1131	1126	1128
$^5D_0$	17261	17261	17257	17251

those assigned to $[Eu(2)(NO_3)_2L_A]^+$ [5], although the crystal field levels (*Table 5*) are clearly different, which examplifies the sensitivity of the luminescent probe technique to conformational differences of the ligand. The two other cationic spectra reported in *Fig. 9*, C_b and C_c, are assigned to weakly populated secondary sites, by analogy with P_b.

A population analysis of the different metal ion sites was performed using the magnetic dipole $^5D_0 \rightarrow {}^7F_1$ transition, the oscillator strength of which is independent of the Eu environment [2][22]. The contribution of $[Eu(NO_3)_5]^{2-}$ to the $^5D_0 \rightarrow {}^7F_1$ transition in the spectrum obtained under broad-band excitation of all the Eu^{III} ions to the $^5L_6$ level is 31% (28% P_a and 3% P_b), a value close to the expected one (33%). The cationic species $[Eu(NO_3)_2L_B]^+$ contribute 69%: 62% for C_a (C_{a1} and C_{a2}), 3% for C_b, and 4% C_c. It, therefore, appears that sites P_b, C_b, and C_c are minor species present in the crystal. Two assumptions can be made to explain their origin. The first one has been given above and refers to crystal defects. The other one is that $[Eu(NO_3)_2L_B]_2[Eu(NO_3)_5]$ includes some 10% of complex moieties containing another isomer of the crown ether. If this were true, isomer *A* would be barred, since, for instance, the energies of the $^5D_0 \leftarrow {}^7F_0$ transitions corresponding to C_b and C_c fall outside the range reported for the compound with the *A* isomer. Moreover, the crystal field levels reported in *Table 5* do not correspond to those reported for the *A* isomer [5].

Luminescence lifetimes of the $Eu(^5D_0)$ level have been measured under selective excitation for samples of pure $[Eu(NO_3)_2L_B]_2[Eu(NO_3)_5]$ and of the Eu-doped (2%) Gd complex (*Table 6*). Lifetimes are less sensitive to changes in the chemical environment than crystal-field splittings, and no distinction could be made between the various $[Eu(NO_3)_5]^{2-}$ and $[Eu(NO_3)_2L_B]^+$ species. For the latter, there is no difference between the lifetimes measured on the Eu-containing and Eu-doped Gd complex cations. Moreover,

Table 6. *Lifetimes of the $Eu(^5D_0)$ Level in $[Eu(NO_3)_2L_B][Eu(NO_3)_5]$ and in the Eu-Doped* (2%) *Gd Analogue, Along with Comparison Data.* Lifetimes are averages of 6–8 determinations.

Species		Lifetimes [ms]	
		77 K	295 K
$[Eu(NO_3)_2L_A]^+$	100% [5]	1.57 ± 0.05	1.46 ± 0.01
$[Eu(NO_3)_2L_B]^+$	100% [a]	1.62 ± 0.03	1.45 ± 0.03
	2% [a]	1.60 ± 0.03	1.40 ± 0.09
$[Eu(NO_3)_5]^{2-}$	L_A, 100% [5]	1.09 ± 0.02	n.a.
	L_B, 100% [b]	1.17 ± 0.04	1.25 ± 0.07
	L_B, 2% [b]	1.02 ± 0.04	0.99 ± 0.03
	solution [23][c]	n.a.	1.25 ± 0.05

[a] λ_{exc} = 579.3 (C_a), 579.5 (C_b), or 579.7 (C_c) nm; selective analysis on both $^5D_0 \rightarrow {}^7F_1$ and $^5D_0 \rightarrow {}^7F_2$.
[b] λ_{exc} = 580.0 (P_b) or 580.2 (P_a) nm; selective analysis on $^5D_0 \rightarrow {}^7F_J$ (J = 1, 2 and 4).
[c] $(Me_4N)_2[Eu(NO_3)_5]$ 0.05M in MeCN.

the temperature dependence is small, which is indicative of the participation of a large number of vibrational quanta in the non-radiative process [5]. For $[Eu(NO_3)_5]^{2-}$, the situation is similar, except for the shorter lifetime recorded with the Eu-doped Gd moiety, pointing to some radiative energy transfer taking place in the pure Eu compound and lengthening the lifetime.

5. Conclusion. – This study confirms the sensitivity of the Eu^{III} ion as luminescent probe in solid state structural analysis. Despite similar coordination environments of the metal ions in the complex cations $[Eu(NO_3)_2L_B]^+$, different spectra could be identified for Eu(1) and Eu(2). Moreover, the detailed analysis of the excitation and emission spectra revealed the presence of secondary anionic and cationic sites (population *ca.* 10%) which could not be evidenced by the X-ray analysis. These sites correspond to molecules having a conformation slightly different from that of the main species.

This research is supported through a grant from the *Swiss National Science Foundation*. We thank the *Fondation Herbette* (Lausanne) for the gift of spectroscopic equipment.

REFERENCES

[1] J.-C.G. Bünzli, J.M. Harrowfield, in 'Calixarenes, a Versatile Class of Macrocyclic Compounds', Eds. V. Böhmer and J. Vicens, Kluwer Academic Press, Amsterdam, in press.
[2] 'Lanthanide Probes in Life, Chemical and Earth Sciences', Eds. G.R. Choppin and J.-C.G. Bünzli, Elsevier Science Publ. B.V., Amsterdam, 1989.
[3] J.-C.G. Bünzli, B. Klein, G. Chapuis, K.J. Schenk, *Inorg. Chem.* **1982,** *21,* 808.
[4] J.-C.G. Bünzli, G.A. Leonard, D. Plancherel, G. Chapuis, *Helv. Chim. Acta* **1986,** *69,* 288.
[5] D. Plancherel, Linpei Jin, R. Massara, J.-C.G. Bünzli, *Helv. Chim. Acta* **1987,** *70,* 1807.
[6] J.-C.G. Bünzli, G.-O. Pradervand, *J. Chem. Phys.* **1986,** *85,* 2489.
[7] F. Nicolò, D. Plancherel, G. Chapuis, J.-C.G. Bünzli, *Inorg. Chem.* **1988,** *27,* 3518.
[8] J.-C.G. Bünzli, D. Plancherel, G.-O. Pradervand, *J. Phys. Chem.* **1989,** *93,* 980.
[9] P. Guerriero, P.A. Vigato, J.-C.G. Bünzli, E. Moret, *J. Chem. Soc., Dalton Trans.* **1990,** 647.
[10] M. Mercer, M.R. Truter, *J. Chem. Soc., Dalton Trans.* **1973,** 2215.
[11] J.-C.G. Bünzli, in 'Handbook on the Physics and Chemistry of Rare Earths', Eds. K.A. Gschneidner, Jr. and L. Eyring, Elsevier Science Publ. B.V., Amsterdam, 1987, Vol. 9, Chapt. 60.
[12] M.E. Harman, F.A. Hart, M.B. Hursthouse, G.P. Moss, P.R. Raithby, *J. Chem. Soc., Chem. Commun.* **1976,** 396.
[13] F. Nicolò, D. Plancherel, J.-C.G. Bünzli, G. Chapuis, *Helv. Chim. Acta* **1987,** *70,* 1798.
[14] Y. Fan, C. Shen, F. Wang, Z. Jin, Y. Gao, J. Ni, *Mol. Sci. Chem. Res. (China)* **1984,** *3,* 371.
[15] R.M. Izatt, B.L. Haymore, J.S. Bradshaw, J.J. Christensen, *Inorg. Chem.* **1975,** *14,* 3132.
[16] 'International Tables of Crystallography', Kynoch Press, Birmingham, 1974, Vol. IV.
[17] G. Sheldrick, SHELX76 Computing System, University of Cambridge, 1976; adapted locally by F. Nicolò.
[18] M. Nardelli, *Computer Chem.* **1983,** *7,* 95.
[19] J.-C.G. Bünzli, B. Klein, G.-O. Pradervand, P. Porcher, *Inorg. Chem.* **1983,** *22,* 3763.
[20] R.D. Shannon, *Acta Crystallogr., Sect. A* **1976,** *32,* 751.
[21] F. Nicolò, J.-C.G. Bünzli, G. Chapuis, *Acta Crystallogr., Sect. C* **1988,** *44,* 1733.
[22] P. Porcher, P. Caro, *J. Luminesc.* **1980,** *21,* 207.
[23] J.-C.G. Bünzli, J.-R. Yersin, *Inorg. Chim. Acta* **1984,** *94,* 301.